

## In situ synchrotron radiation photoelectron spectroscopy study of the oxidation of the Ge(100)-2 × 1 surface by supersonic molecular oxygen beams

Akitaka Yoshigoe, Yuden Teraoka, Ryuta Okada, Yoichi Yamada, and Masahiro Sasaki

Citation: *The Journal of Chemical Physics* **141**, 174708 (2014); doi: 10.1063/1.4900633

View online: <http://dx.doi.org/10.1063/1.4900633>

View Table of Contents: <http://scitation.aip.org/content/aip/journal/jcp/141/17?ver=pdfcov>

Published by the [AIP Publishing](#)

---

### Articles you may be interested in

[Kinetic study of GeO disproportionation into a GeO<sub>2</sub>/Ge system using x-ray photoelectron spectroscopy](#)  
*Appl. Phys. Lett.* **101**, 061907 (2012); 10.1063/1.4738892

[Carbon contamination and oxidation of Au surfaces under extreme ultraviolet radiation: An x-ray photoelectron spectroscopy study](#)  
*J. Vac. Sci. Technol. B* **30**, 041603 (2012); 10.1116/1.4737160

[Nanoscale oxidation of Cu\(100\): Oxide morphology and surface reactivity](#)  
*J. Chem. Phys.* **126**, 034703 (2007); 10.1063/1.2424932

[Kinetics of the CO oxidation reaction on Pt\(111\) studied by in situ high-resolution x-ray photoelectron spectroscopy](#)  
*J. Chem. Phys.* **120**, 7113 (2004); 10.1063/1.1669378

[The thermal chemistry of saturated layers of acetylene and ethylene on Ni\(100\) studied by in situ synchrotron x-ray photoelectron spectroscopy](#)  
*J. Chem. Phys.* **119**, 1710 (2003); 10.1063/1.1582432

---



# ***In situ* synchrotron radiation photoelectron spectroscopy study of the oxidation of the Ge(100)-2 × 1 surface by supersonic molecular oxygen beams**

Akitaka Yoshigoe,<sup>1,a)</sup> Yuden Teraoka,<sup>1,2</sup> Ryuta Okada,<sup>1,3</sup> Yoichi Yamada,<sup>3</sup> and Masahiro Sasaki<sup>3</sup>

<sup>1</sup>Quantum Beam Science Center, Japan Atomic Energy Agency, 1-1-1 Kouto, Sayo-cho, Hyogo 679-5148, Japan

<sup>2</sup>University of Hyogo, 3-2-1 Kouto, Kamigori-cho, Ako-gun, Hyogo 678-1297, Japan

<sup>3</sup>University of Tsukuba, 1-1-1 Tennodai, Tsukuba, Ibaraki 305-8573, Japan

(Received 12 June 2014; accepted 16 October 2014; published online 5 November 2014)

*In situ* synchrotron radiation photoelectron spectroscopy was performed during the oxidation of the Ge(100)-2 × 1 surface induced by a molecular oxygen beam with various incident energies up to 2.2 eV from the initial to saturation coverage of surface oxides. The saturation coverage of oxygen on the clean Ge(100) surface was much lower than one monolayer and the oxidation state of Ge was +2 at most. This indicates that the Ge(100) surface is so inert toward oxidation that complete oxidation cannot be achieved with only pure oxygen (O<sub>2</sub>) gas, which is in strong contrast to Si surfaces. Two types of dissociative adsorption, trapping-mediated and direct dissociation, were confirmed by oxygen uptake measurements depending on the incident energy of O<sub>2</sub>. The direct adsorption process can be activated by increasing the translational energy, resulting in an increased population of Ge<sup>2+</sup> and a higher final oxygen coverage. We demonstrated that hyperthermal O<sub>2</sub> beams remarkably promote the room-temperature oxidation with novel atomic configurations of oxides at the Ge(100) surface. Our findings will contribute to the fundamental understanding of oxygen adsorption processes at 300 K from the initial stages to saturated oxidation. © 2014 AIP Publishing LLC. [<http://dx.doi.org/10.1063/1.4900633>]

## **I. INTRODUCTION**

Germanium (Ge) and its oxides play a crucial role in a wide variety of fields, such as electronics, fiber optics, infrared devices, radiation detectors, and catalysts for polymer synthesis. In particular, Ge shows excellent characteristics as a promising substitute material for Si in next-generation metal–insulator–semiconductor field-effect transistor (MISFET) devices owing to its high carrier mobility, narrow band gap, and low process temperature.<sup>1</sup> In the development of Ge-based MISFET devices, controlled formation of the surface oxide in a wide variety of ways is important for precise fabrication of dielectric/Ge interfaces.<sup>2–13</sup> Therefore, atomic-level understanding of the oxidation of Ge surfaces, especially in the monolayer or sub-monolayer region, is a key research issue. However, the fundamental aspects of the oxidation reaction of Ge surfaces are not well understood, which is in strong contrast to Si surfaces.

Investigation of the surface oxides of Ge has mainly focused on two extreme limits: native oxides in air and the initial stages of oxidation under ultra-high vacuum (UHV) conditions. The native oxides of both Ge and Si exhibit oxidation states up to +4.<sup>14</sup> However, it is widely recognized that Ge oxides in the atmosphere are much less thermally stable and water-soluble than Si oxides. To clarify the detailed nature of

the surface oxides of Ge, fundamental studies focusing on the oxidation of single-crystal Ge surfaces by pure oxygen gas (O<sub>2</sub>) have become increasingly important.

The fundamental aspects of the oxidation reaction at the single-crystal faces of Ge using O<sub>2</sub> are not fully understood. In 1982, Surnev and Tikhov conducted experimental studies on the chemisorption mechanisms of O<sub>2</sub> on the Ge(100) surface.<sup>15</sup> Subsequently, Hansen and Hudson<sup>16</sup> performed molecular beam scattering measurements and found that the translational energy of incident oxygen ( $E_t$ ) affects the initial sticking probability. These investigations found two oxygen adsorption processes on Ge surfaces, trapping-mediated and direct adsorption, similar to Si surfaces. The sticking probability for Ge surfaces has also been found to be considerably smaller than that for Si surfaces. However, although these studies suggest that molecular beams could be useful to investigate surface oxidation, the oxygen adsorption sites remain unclear.

The oxygen adsorption sites on the Ge(100) surface have been investigated by experimental and theoretical studies. Fukuda *et al.*<sup>17</sup> used ultraviolet photoelectron spectroscopy (UPS) and scanning tunneling microscopy (STM) to investigate the products of dissociative chemisorption in the early stages of oxidation for a clean Ge(100)-2 × 1 surface. Soon *et al.*<sup>18</sup> used both high-resolution electron energy loss spectroscopy (HREELS) and computer simulations based on density functional theory (DFT) to study the dissociative chemisorption pathways of O<sub>2</sub> to form the initial products on

<sup>a)</sup> Author to whom correspondence should be addressed. Electronic mail: [yoshigoe@spring8.or.jp](mailto:yoshigoe@spring8.or.jp).

the Ge(100)- $2 \times 1$  surface. Grassman *et al.*<sup>19</sup> confirmed the dissociative adsorption sites for oxygen on the Ge(100)- $2 \times 1$  surface using STM observations and DFT simulations. These findings under low oxygen exposure conditions are supported by computational studies.<sup>20,21</sup> Fleischmann *et al.*<sup>22</sup> reported a detailed study of the oxygen adsorption sites revealed by STM and electron diffraction experiments, describing the favorable oxygen adsorption site at moderate O<sub>2</sub> exposure. Despite the considerable effort to study oxidation of Ge(100) surfaces, there is a lack of information on the chemical analysis of oxidized Ge surfaces and the dependence of the absolute oxygen amount, which are relevant in the characterization of oxide structures. Additionally, little attention has been paid to the experimental clarification of oxides induced by not only thermal-O<sub>2</sub> but also molecular O<sub>2</sub> beams, as examined by Hansen and Hudson.<sup>16</sup>

It is well known that core-level photoelectron spectroscopy is a powerful tool to give detailed information about the chemical environment and oxidation states of oxides at solid surfaces.<sup>5-9,23-27</sup> Schmeisser *et al.*<sup>28</sup> and Kuhr and Ranke<sup>29</sup> reported Ge 3*d* core-level spectra for various oxygen exposures to a Ge(100) surface. Two chemically shifted components of Ge 3*d*, corresponding to Ge atoms with one or two oxygen ligands, were debated. These findings are particularly interesting as the results of the chemical analysis of oxidized Ge(100) surfaces. However, although the peak positions attributed to Ge oxidation states were described in their core-level spectra, no detailed oxide-related components, which are widely reported in silicon oxidation studies,<sup>23-27</sup> were given as a function of the oxygen coverage in both papers.

There is a lack of reliable structural information about Ge oxides after oxidation using O<sub>2</sub> for the clean Ge(100)- $2 \times 1$  surface. Additionally, time-evolution of oxides from the initial oxidation stages to saturation depending on O<sub>2</sub> incident energies have not been fully investigated. In general, hyperthermal energetic O<sub>2</sub> is a candidate to promote oxygen chemisorption and form unique oxide structures.<sup>30,31</sup> In fact, we previously demonstrated the usefulness of experiments using synchrotron radiation X-ray photoelectron spectroscopy (SR-XPS) in conjunction with supersonic O<sub>2</sub> beams to clarify oxide structures depending on  $E_i$ .<sup>26,32</sup> Thus, we believe that supersonic O<sub>2</sub> beams could possibly facilitate novel oxidation at Ge surfaces and select the chemical compositions of Ge oxides via a novel reaction pathway. However, there has been little discussion on these issues for oxidation of Ge(100) surfaces from a fundamental viewpoint.

This paper presents a rigorous analysis of oxides after exposure of a clean Ge(100)- $2 \times 1$  surface to pure O<sub>2</sub> gas using thermal-O<sub>2</sub> (26 meV) or supersonic O<sub>2</sub> beams with various incident energies. Here, we investigated oxygen adsorption processes at room temperature because passive oxidation takes place without both O<sub>2</sub> and GeO desorption involved in the decomposition Ge oxides. We performed *in situ* SR-XPS measurements during surface oxidation from an initial stage to the maximum coverage of the surface oxides. The initial sticking probability of the oxygen molecule on Ge(100) was measured for a wide range of incident energies.

## II. EXPERIMENTS

All of the experiments were performed in UHV using SUREAC2000<sup>25-27,32</sup> constructed at the soft X-ray beamline, BL23SU,<sup>33</sup> at SPring-8, Hyogo, Japan. The SUREAC2000 is equipped with a supersonic O<sub>2</sub> beam generator and hemispherical electron energy analyzer (EA125-5MCD, Omicron Nanotechnology GmbH, Taunusstein, Germany) and low-energy electron diffraction (LEED) facilities.

A Sb-doped Ge(100) substrate with a resistivity of 0.1–0.6  $\Omega$  cm was used in this study. The surface preparation was performed by chemical treatment and *in situ* treatment in the UHV apparatus. The wet treatment used in this study was essentially the same as the method already established by Prabhakaran and Ogino.<sup>34</sup> In UHV with base pressure greater than  $2 \times 10^{-8}$  Pa, conventional cycles of Ar<sup>+</sup>-ion sputtering (0.5 keV) with annealing (773 K) and subsequent flush annealing close to 1200 K for about 5 min were performed several times. After the cleaning procedure, a clear diffraction pattern from the double-domain ( $2 \times 1$ ) superstructure of the Ge(100) surface was readily observed. No impurities, such as carbon and molybdenum atoms, were detected by high-sensitive SR-XPS measurements. Furthermore, a component attributed to up-atoms of the Ge–Ge dimer was clearly observed at the lower binding energy side of the Ge 3*d* bulk peak.

*In situ* oxidation experiments were performed at a substrate temperature of 300 K. Supersonic O<sub>2</sub> beams<sup>35-37</sup> were generated by adiabatic expansion of diluted O<sub>2</sub> gas with He gas, and further mixing with and without Ar gas through a nozzle. We controlled the  $E_i$  value of the O<sub>2</sub> molecular beam by the gas mixing-ratio and the nozzle temperature. The maximum energy of the O<sub>2</sub> beam was 2.33 eV with a nozzle temperature of 1400 K. The  $E_i$  values used in this paper were calculated values.<sup>26,27,38,39</sup> Here, it should be noted that in this study no difference was found with changing nozzle temperature. Thus, we considered that the influence of vibrationally excited O<sub>2</sub> species on oxidation was negligibly small in this reaction system. For the minimum energy of 26 meV, we used effusive oxygen, so-called thermal-O<sub>2</sub>, substantialized by backfilling of oxygen gas, which was introduced with a variable-leak valve ( $< 2 \times 10^{-3}$  Pa). The flux density of the supersonic O<sub>2</sub> beams was determined from the partial pressure measurements of O<sub>2</sub>, He, and Ar gases. Each partial pressure was measured using the quadrupole mass analyzer equipped along the supersonic O<sub>2</sub> molecular beam axis. The typical flux density of the molecular beams was in the order of  $10^{14}$  molecules cm<sup>-2</sup> s<sup>-1</sup>, and the variation was less than 1%. The flux density of thermal-O<sub>2</sub> was calculated by the Hertz-Knudsen equation. The substrate surfaces were exposed to supersonic O<sub>2</sub> beams at an incident angle of 10° from surface normal directions. The take-off angle of photoelectrons for every oxidation was 60° from the surface normal directions. Note that, the vacuum gauges were located on the far backside of the sample surface to avoid the effects of the atomic oxygen created by its hot-filament during surface oxidation.<sup>15,28</sup>

Circularly polarized synchrotron-light of 669.7 eV was used to record the Ge 3*d* and O 1*s* photoelectron spectra. The experimental overall energy resolution for the photoelectron

spectra was greater than 250 meV. Here, it should be noted that the influence of high flux photon irradiation on oxygen dissociation was negligible because no difference between oxidation with and without continuous illumination of synchrotron radiation light was observed at a certain dose. Furthermore, we are convinced that the decomposition of surface oxides by synchrotron radiation was negligible because no changes of the photoelectron spectra were observed after synchrotron radiation light illumination in the absence of O<sub>2</sub> gas.

### III. RESULTS AND DISCUSSION

First, we will discuss the uptake of oxygen on the clean Ge(100)-2 × 1 surface by the changes in the O 1s spectra. Figure 1 shows the change in the surface oxygen coverage determined from the O 1s intensity as a function of O<sub>2</sub> dose for incident energies of 26 meV and 2.2 eV. The dose value indicated in this paper was obtained from the product of oxidation time and O<sub>2</sub> flux density. In this study, we carefully calibrated the oxygen coverage on the Ge(100) surface by referring to the results of oxygen uptake on the Si(111)-7 × 7 surface, where the relationship between the oxygen coverage and the intensity of the O 1s peak is well-understood.<sup>25–27</sup> This careful calibration allows us to assess the oxygen coverage in monolayer units (ML; 1 ML = 6.19 × 10<sup>14</sup> cm<sup>-2</sup>, corresponding to the density of Ge atoms on the Ge(100)-1 × 1 surface). It was found that the final oxygen coverage was dependent on the incident energy of the oxygen, suggesting that the oxidation process can be activated by the translational energy of the O<sub>2</sub> molecules. It is also important to note that the saturated oxygen coverages were as small as 0.30 and 0.36 ML for incident energies of 26 meV and 2.2 eV, respectively. The saturation coverages were found to be much

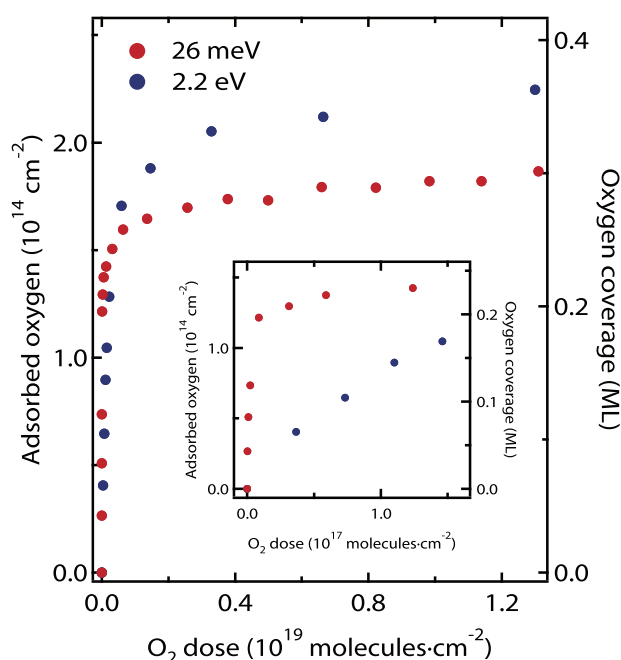


FIG. 1. Oxygen uptake curves of Ge(100)-2 × 1 surface oxidation at 300 K by thermal-O<sub>2</sub> ( $E_i = 26$  meV) and supersonic O<sub>2</sub> beams ( $E_i = 2.2$  eV). The inset shows the enlarged plots of the uptake curves to highlight the early stage of oxidation.

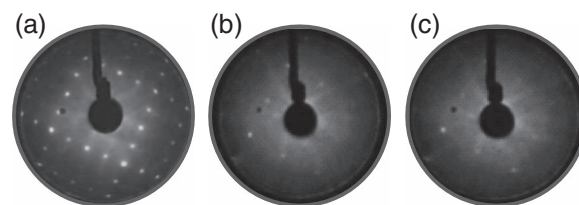


FIG. 2. Low-energy electron diffraction (LEED) images: (a) before oxidation and after saturated oxidation of the Ge(100)-2 × 1 surface at 300 K by (b) thermal-O<sub>2</sub> ( $E_i = 26$  meV) and (c) supersonic O<sub>2</sub> beams ( $E_i = 2.2$  eV).

smaller than those on the Si(111) surface, where the final coverages are up to ~0.9 and ~1.5 ML for incident energies of 26 meV and 2.2 eV, respectively.<sup>26</sup> The fact that the final oxygen coverage can increase with increasing incident energy of oxygen indicates that a new adsorption pathway may occur, resulting in novel oxide structures on Ge surfaces.

Figure 2 shows LEED images before and after oxidation of the Ge(100) surface. The LEED patterns for incident energies of both 26 meV and 2.2 eV show clear 1 × 1 spots even for the saturated surface, as shown in Figs. 2(b) and 2(c). Bulk 1 × 1 spots suggest that oxygen molecules adsorb on the surface only destroying the surface Ge–Ge dimer structures<sup>22</sup> and that the oxygen coverage is low, which is consistent with the results revealed by the quantitative uptake measurements as shown in Fig. 1. It is evident from our results that the Ge(100)-2 × 1 surface seems to be quite inert toward oxidation, which is in sharp contrast to the case of Si surfaces. The remaining 1 × 1 patterns observed even with small coverages at saturation of uptake, as shown in Fig. 1, indicate that the variation of the electronic structures caused by oxygen adsorption probably results in the destruction of Ge–Ge dimers rather than them remaining intact to minimize surface energy. This electronic-structural change may be related to the low coverage at saturation and the decrease of the initial sticking probability caused by the presence of oxygen and impurities as shown later.

In the inset of Fig. 1, we show enlarged plots of the uptake curves. The initial slope is much steeper in the case of lower translational energy, suggesting that the initial oxygen adsorption processes are highly dependent on the translational energy. From the initial slope of the oxygen uptake, we determined the initial sticking probability,  $s_0$ . Figure 3 shows the initial sticking probability of O<sub>2</sub> for the Ge(100)-2 × 1 surface at 300 K as a function of  $E_i$ . The initial sticking probability for oxygen with 26 meV was a few orders of magnitude greater than values reported by other groups.<sup>15–17</sup> This large difference is most likely because of the cleanliness of the surface. We observed that the presence of a small amount of contamination detected by SR-XPS can greatly inhibit oxidation, even for the high incident energy oxygen used in this study.<sup>40</sup> With increasing incident energy, the initial sticking probability rapidly decreased. This trend is similar to that observed for Si oxidation<sup>26,27,30</sup> and is clear proof of the trapping-mediated dissociation process. The presence of the trapping-mediated process has been recently predicted by DFT calculations considering the spin-triplet ground state of oxygen.<sup>21</sup> The experimental data shown here strongly support the theoretical



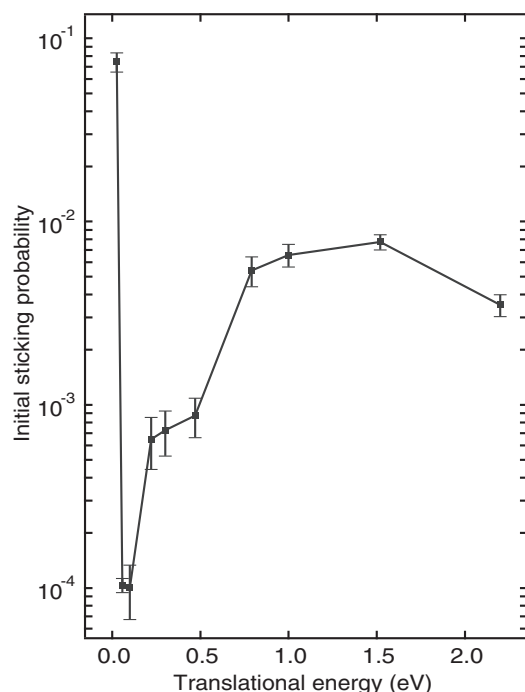


FIG. 3. Translational energy dependence of initial sticking probability of  $O_2$  for the Ge(100)- $2 \times 1$  surface at 300 K.

prediction. The dominance of the trapping-mediated process in the low incident energy region can also explain the fact that a cleaner surface exhibits higher reactivity than other reported values.<sup>15–17</sup> After the rapid decrease of  $s_0$  with  $E_t$ ,  $s_0$  started to increase with further increase of  $E_t$ . This observation suggests the onset of the direct-activated chemisorption process of impinging oxygen with higher translational energies of oxygen. Therefore, it is likely that the emergence of this process opens a new reaction pathway resulting in the increased final oxygen coverage. To confirm the hypothesis of the onset of the new reaction activated by the translational energy, we determined the chemical nature of the surface oxidation products formed with different translational energies. Figure 4 shows the Ge 3d core-level photoelectron spectra of the oxygen-saturated surfaces formed by oxygen with  $E_t$  values of 26 meV and 2.2 eV. To investigate the difference in the suboxide peaks, the signal intensities were normalized by the intensity of the Ge 3d<sub>5/2</sub> bulk peak (Fig. 4(a)). The horizontal axis shows the relative binding energies with respect to the Ge 3d<sub>5/2</sub> bulk peak position. It was found that photoelectron suboxide peaks are present in both cases, and the relative intensity of the suboxide peaks are considerably larger for the oxides formed with 2.2 eV  $O_2$ . Here we analyzed the intensity of the suboxide peaks of the spectra by curve-fitting analysis as follows. Before the curve-fitting analysis, we subtracted the Ge 3d<sub>3/2</sub> component from the spectra shown in Fig. 4(a) through a deconvolution process.<sup>41</sup> Figure 4(b) shows the Ge 3d<sub>5/2</sub> core-level photoelectron spectra after subtraction of the Ge 3d<sub>3/2</sub> component, in which the signals of the suboxides become clearer in both spectra. To resolve the oxide-related components observed at the higher binding energy side of the bulk peak, the Ge 3d<sub>5/2</sub> spectral line shape was analyzed by a curve-fitting procedure using

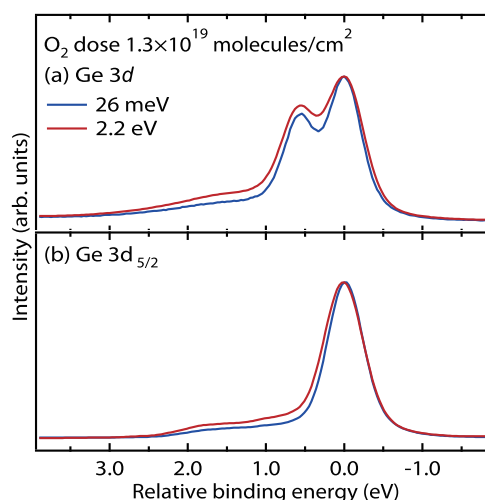


FIG. 4. (a) Comparison of Ge 3d core-level photoelectron spectra of the oxygen-saturated surface for oxygen with  $E_t$  of 26 meV and 2.2 eV. (b) Ge 3d<sub>5/2</sub> core-level photoelectron spectra after the subtraction of the 3d<sub>3/2</sub> component from (a) through the de-convolution process. The signal intensities were normalized by the Ge 3d<sub>5/2</sub> bulk peak intensity. The horizontal axis shows the relative binding energy with respect to the Ge 3d<sub>5/2</sub> bulk peak position.

symmetric Voigt functions constructed by the convolution of Lorentzian and Gaussian functions. The Lorentzian full width at half maximum (LW) of 150 meV was used for all components according to Eriksson and Uhrberg.<sup>42</sup> The value of the Gaussian full width at half maximum (GW) was separately determined for each single peak profile. In addition to the bulk component, four components were required for both spectra to obtain a reasonable fit. One component originated from subsurface Ge atoms at  $-0.2$  eV<sup>42</sup> and the other component ( $\gamma$ ) was located at  $-0.5$  eV. The component  $\gamma$  seems to originate from the Ge–Ge dimer at the residual unoxidized area on the surface<sup>42</sup> and/or can be assigned to the oxide-related component normally observed in the oxidation of Si surfaces.<sup>25,43–45</sup> The positions of the components related to suboxide states such as Ge<sup>1+</sup> and Ge<sup>2+</sup> were set to the positions reported by Schmeisser *et al.*<sup>28</sup> Figure 5 shows the results of curve-fitting analysis, and the parameters obtained from the curve-fitting analysis are shown in Table I. Our analysis clearly revealed the Ge<sup>1+</sup> and Ge<sup>2+</sup> oxidation states at core-level shifts of 0.81 and 1.71 eV, respectively. Only the two distinctive oxide components Ge<sup>1+</sup> and Ge<sup>2+</sup> were identified even after saturation. This is completely different from what is observed in the oxidation of clean single-crystal Si surfaces, such as Si(100) and Si(111) under the same conditions, where oxidation states up to Si<sup>4+</sup> are generated.<sup>25,27,43,44</sup> This result clearly indicates that the Ge(100)- $2 \times 1$  surface is quite inert toward oxidation by pure oxygen gas unlike the case of Si oxides. The results obtained in this study seem to be considerably different from the reported results for high pressure<sup>11</sup> and atmospheric oxidation,<sup>14</sup> where the Ge<sup>4+</sup> state was clearly identified. Since the present results suggest that Ge<sup>4+</sup> cannot be formed by the reaction of pure oxygen gas at room temperature, it is likely that several processes play a role in progressing oxidation in the other methods.<sup>11,14</sup> One possible reason for the production

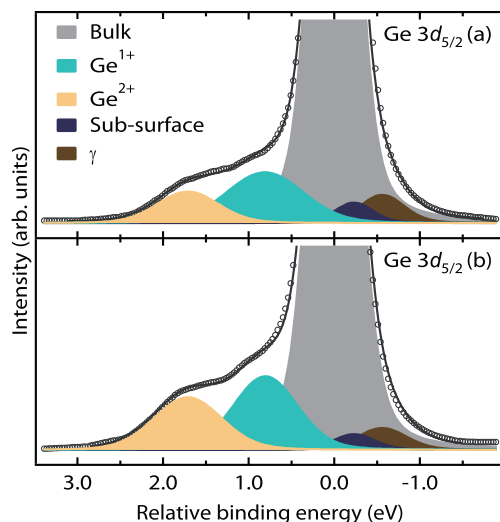


FIG. 5. Curve-fitting analysis of Ge  $3d_{5/2}$  spectra at saturated oxidation for the Ge(100) surface dosed with  $1.3 \times 10^{19}$  molecules  $\text{cm}^{-2}$  for  $E_i$  values of (a) 26 meV and (b) 2.2 eV.

of Ge oxides with high oxidation states is that oxygen diffusion into oxides is dominant at high temperature.<sup>46</sup> This oxygen transport mechanism involved in the thermal Ge oxidation may facilitate oxidation and prevent GeO desorption relevant to  $\text{GeO}_2$  decomposition. The kinetic balance between the growth of oxides and the GeO desorption processes seems to be a key mechanism under high-temperature and low-pressure oxidation, resulting in the difference between our experimental results and previous high-pressure work. Further studies should focus on this subject. Another possible reason for the progress of oxidation in the atmospheric conditions is the involvement of other reactants, such as vapor-water.<sup>14</sup> Indeed, we confirmed the  $\text{Ge}^{4+}$  component for sample surfaces introduced from the atmosphere prior to the oxidation experiments (not shown in this paper). We are currently in the progress of investigating the chemical analysis of surface oxides fabricated in the atmospheric conditions.

We also found that the  $\text{Ge}^{2+}/\text{Ge}^{1+}$  ratio evaluated from the intensities was  $\sim 0.5$  for oxidation by 26 meV  $\text{O}_2$ , whereas it was  $\sim 0.75$  for oxidation by 2.2 eV  $\text{O}_2$  beams. We thus considered that the translational energy can activate the direct dissociation process, increasing the population of  $\text{Ge}^{2+}$  and thus the final oxygen coverage. Figure 6 shows the dose dependence of suboxide intensities ( $\text{Ge}^{1+}$  and  $\text{Ge}^{2+}$ ). The intensi-

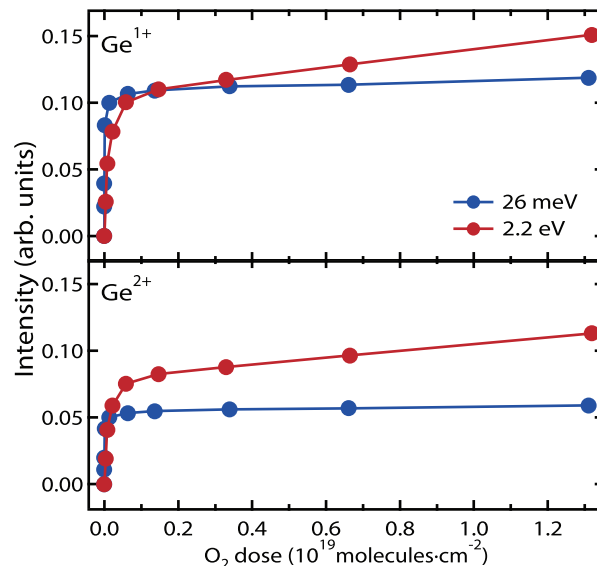


FIG. 6. Dose dependence of the suboxide intensities of  $\text{Ge}^{1+}$  and  $\text{Ge}^{2+}$ .

ties of  $\text{Ge}^{1+}$  and  $\text{Ge}^{2+}$  simultaneously increased with increasing dose. Furthermore, the  $\text{Ge}^{2+}/\text{Ge}^{1+}$  ratios were constant from the initial stage of oxidation to saturation. This is also different from the oxidation of Si surfaces, where oxidation products with higher oxidation states appear after the formation of oxides with lower oxidation states.<sup>25,43,44</sup>

From the above results, we were able to determine the adsorption sites of oxygen on the surface and the growth processes of oxides on the Ge(100)- $2 \times 1$  surface. Our experiments confirmed that the  $\text{Ge}^{2+}/\text{Ge}^{1+}$  ratio was  $\sim 0.5$  for oxidation using  $\text{O}_2$  with suitable energy. This clearly indicates the formation of type A oxides, as shown in Fig. 7. Dissociated oxygen chemisorbs at the bridge site and the backbond site of the Ge-Ge dimer to form the type A structure. This structure has one  $\text{Ge}^{2+}$  atom and two  $\text{Ge}^{1+}$  atoms, ideally resulting in a  $\text{Ge}^{2+}/\text{Ge}^{1+}$  ratio of 0.5. Previous studies of Ge(100)- $2 \times 1$  oxidation using thermal- $\text{O}_2$  by HREELS and DFT reported by Soon *et al.*<sup>18</sup> and STM combined with DFT reported by Grassman *et al.*<sup>19</sup> also suggested that the most plausible structure is the type A oxide. Our results from *in situ* chemical analysis using SR-XPS agree with these previous results. However, we found that the energetic  $\text{O}_2$  beam induces oxides with a  $\text{Ge}^{2+}/\text{Ge}^{1+}$  ratio of  $\sim 0.75$ , indicating the formation of a different oxide. This new oxide is possibly of the form of the type B structure shown in Fig. 7. In this phase, a further oxygen atom adsorbs to an opposite backbond site, increasing the amount of  $\text{Ge}^{2+}$ . The observed  $\text{Ge}^{2+}/\text{Ge}^{1+}$  ratio

TABLE I. Energy positions, full width at half maximum (FWHM) of Gaussian functions, and area intensities of Ge  $3d$  components obtained from curve-fitting analysis.

		Bulk	$\text{Ge}^{1+}$	$\text{Ge}^{2+}$	Subsurface	$\gamma$
26 meV	E (eV)	0	0.81	1.71	-0.23	-0.56
	GW (eV)	0.439	0.976	0.751	0.439	0.527
	Intensity	1	0.127	0.064	0.027	0.043
2.2 eV	E (eV)	0	0.81	1.71	-0.23	-0.56
	GW (eV)	0.495	0.809	0.856	0.495	0.594
	Intensity	1	0.160	0.120	0.023	0.037

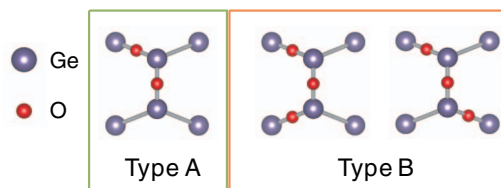


FIG. 7. Ball-stick models of the oxygen adsorption sites on the Ge(100)- $2 \times 1$  surface, which are formed by oxygen with  $E_i$  values of 26 meV (type A) and 2.2 eV (type B).

of  $\sim 0.75$  indicates that type **A** and type **B** structures spontaneously coexist a ratio of type **A**:type **B** = 1:1. Taking into account the change of the  $\text{Ge}^{2+}/\text{Ge}^{1+}$  ratio with  $\text{O}_2$  dose, the type **A** and type **B** oxides probably simultaneously increase. This model of oxide growth on the  $\text{Ge}(100)\text{-}2 \times 1$  surface differs from that at Si surfaces, where the amounts of several types of oxides with higher oxidation states increase with increasing dose.<sup>25,27</sup>

Therefore, our present results show that the oxide layer of Ge exhibits properties that are considerably different from Si oxides. We showed that the  $\text{Ge}(100)$  surface is so inert that it cannot be completely covered with monolayer-thickness  $\text{GeO}_2$  by oxidation with pure  $\text{O}_2$  gas at room temperature, indicating a pressure and temperature gap between our oxidation and other methods.<sup>11,14</sup> Further experimental studies using ambient pressure XPS<sup>47</sup> may be able to fill the pressure gap observed in  $\text{Ge}(100)$  oxidation. In addition, we are confident that our research will serve as a basis for future studies on thermal oxidation using molecular beams. It is also important to investigate other orientations of the surface. The present results suggest that the other low-index surfaces of Ge may also possess unique properties that are worth investigating. On the other hand, a fundamental point of view, the most important result from the present study is the low surface reactivity with oxygen. The low saturation coverage of oxides with low final oxidation states suggests that the oxidation reaction is probably influenced by the presence of a small amount of adsorbed oxygen, resulting in a potential energy barrier for further dissociative adsorption of  $\text{O}_2$  on Ge surfaces. This energy barrier is responsible for the activated adsorption process observed with supersonic  $\text{O}_2$  beams with high translational energy. However, the detailed mechanisms for the formation of the apparent potential energy barrier for not only clean but also oxygen-adsorbed  $\text{Ge}(100)$  surfaces remain unclear.<sup>21</sup> Theoretical studies will be required to obtain detailed physical insight into the origin of  $\text{O}_2$  adsorption.<sup>48–50</sup>

#### IV. SUMMARY

In conclusion, we studied the fundamental aspects of  $\text{O}_2$  chemisorption on the  $\text{Ge}(100)\text{-}2 \times 1$  surface at room temperature by *in situ* X-ray photoelectron spectroscopy using synchrotron radiation, focusing on the dependence of the translational energy of the incident oxygen molecules. It was found that the  $\text{Ge}(100)$  surface was quite inert toward oxidation for not only thermal- $\text{O}_2$  but also hyperthermal  $\text{O}_2$  beams. The final oxygen coverage was lower than 0.4 ML and the final oxidized state was  $\text{Ge}^{2+}$  for all oxidation conditions. These findings are in strong contrast to the case of  $\text{Si}(111)$  oxidation using 26 meV  $\text{O}_2$ , where the oxygen coverage and oxidation state reached 0.9 ML and  $\text{Si}^{4+}$ , respectively. The adsorption sites of oxygen were determined to be the bridge and backbond sites on the surface Ge–Ge dimer. Direct adsorption can take place with high translational energy, facilitating further chemisorption to the backbond site that results in a significant increase in the  $\text{Ge}^{2+}$  state. These results demonstrate control of the chemical composition of Ge oxides on the  $\text{Ge}(100)$  surface at room temperature.

#### ACKNOWLEDGMENTS

This work was partially supported by grants-in-aid from the Ministry of Education, Cultures, Sports, Science and Technology, for Exploratory Research (Grant Nos. 17656239, 19360336, 20360024, and 26420289). We thank the following people for their support of synchrotron radiation operation: Dr. Y. Saitoh and Dr. Y. Fukuda. The authors wish to thank Dr. J. Harries, Dr. M. Tode, Mr. M. Jinno, and Mr. K. Inoue, who gave us much support in the early stages of this work. We are grateful to Mr. T. Nishimura for his technical assistance. The synchrotron radiation experiments were performed at the BL23SU of SPring-8 with the approval of the Japan Synchrotron Radiation Research Institute (JASRI) (Proposal Nos. 2007B3802, 2008A3804, 2008B3804, 2009A3804, 2011A3804, 2011B3802, 2012A3802, 2012B3802, 2013A3802, and 2013B3802).

- <sup>1</sup>M. Houssa, A. Satta, E. Simoen, B. De Jaeger, M. Meuris, M. Caymax, and M. Heyns, in *Germanium Based Technologies: From Materials to Devices*, edited by C. Cleys and E. Simoen (Elsevier, Amsterdam, 2007), p. 233.
- <sup>2</sup>S. Spiga, C. Wiemer, G. Tallarida, G. Scarel, S. Ferrari, G. Seguini, and M. Fanciulli, *Appl. Phys. Lett.* **87**, 112904 (2005).
- <sup>3</sup>S. Rangan, E. Bersch, R. A. Bartynski, E. Garfunkel, and E. Vescovo, *Appl. Phys. Lett.* **92**, 172906 (2008).
- <sup>4</sup>D. Kuzum, T. Krishnamohan, A. J. Pethe, A. K. Okyay, Y. Oshima, Y. Sun, J. P. McVittie, P. A. Pianetta, P. C. McIntyre, and K. C. Saraswat, *IEEE Electron Device Lett.* **29**, 328 (2008).
- <sup>5</sup>X.-J. Zhang, G. Xue, A. Agarwal, R. Tsu, M.-A. Hassan, J. E. Greene, and A. Rockett, *J. Vac. Sci. Technol., A* **11**, 2553 (1993).
- <sup>6</sup>V. Craciun, I. W. Boyd, B. Hutton, and D. Williams, *Appl. Phys. Lett.* **75**, 1261 (1999).
- <sup>7</sup>A. Molle, Md. N. K. Bhuiyan, G. Tallarida, and M. Fanciulli, *Appl. Phys. Lett.* **89**, 083504 (2006).
- <sup>8</sup>A. Delabie, F. Bellenger, M. Houssa, T. Conard, S. V. Elshocht, M. Caymax, M. Heyns, and M. Meuris, *Appl. Phys. Lett.* **91**, 082904 (2007).
- <sup>9</sup>A. Molle, S. Baldovino, S. Spiga, and M. Fanciulli, *Thin Solid Films* **518**, S96 (2010).
- <sup>10</sup>H. Matsubara, T. Sasada, M. Takenaka, and S. Takagi, *Appl. Phys. Lett.* **93**, 032104 (2008).
- <sup>11</sup>C. H. Lee, T. Tabata, T. Nishimura, K. Nagashio, K. Kita, and A. Toriumi, *Appl. Phys. Express* **2**, 071404 (2009).
- <sup>12</sup>M. Yang, R. Q. Wu, Q. Chen, W. S. Deng, Y. P. Feng, J. W. Chai, J. S. Pan, and S. J. Wang, *Appl. Phys. Lett.* **94**, 142903 (2009).
- <sup>13</sup>M. Houssa, G. Pourtois, M. Caymax, M. Meuris, and M. M. Heyns, *Surf. Sci.* **602**, L25 (2008).
- <sup>14</sup>S. K. Sahari, H. Murakami, T. Fujioka, T. Bando, A. Ohta, K. Makiyama, S. Higashi, and S. Miyazaki, *Jpn. J. Appl. Phys.* **50**, 04DA12 (2011).
- <sup>15</sup>L. Surnev and M. Tikhov, *Surf. Sci.* **123**, 505 (1982).
- <sup>16</sup>D. A. Hansen and J. B. Hudson, *Surf. Sci.* **254**, 222 (1991); **292**, 17 (1993).
- <sup>17</sup>T. Fukuda and T. Ogino, *Phys. Rev. B* **56**, 13190 (1997); *Surf. Sci.* **380**, L469 (1997); *Appl. Surf. Sci.* **130–132**, 165 (1998).
- <sup>18</sup>J. M. Soon, C. W. Lim, and K. P. Loh, *Phys. Rev. B* **72**, 115343 (2005).
- <sup>19</sup>T. J. Grassman, S. R. Bishop, and A. C. Kummel, *Surf. Sci.* **602**, 2373 (2008).
- <sup>20</sup>E. J. J. Kirchner and E. J. Baerends, *Surf. Sci.* **311**, 126 (1994).
- <sup>21</sup>X. L. Fan, W. M. Lau, and Z. F. Liu, *J. Phys. Chem. C* **113**, 8786 (2009).
- <sup>22</sup>C. Fleischmann, K. Schouteden, C. Merckling, S. Sioncke, M. Meuris, C. V. Haesendonck, K. Temst, and A. Vantomme, *J. Phys. Chem. C* **116**, 9925 (2012).
- <sup>23</sup>M. V. Gomoyunova and I. I. Pronin, *Tech. Phys.* **49**, 1249 (2004).
- <sup>24</sup>G. L. Lay, V. Y. Aristov, and M. Fontaine, *Prog. Surf. Sci.* **48**, 145 (1995).
- <sup>25</sup>A. Yoshigoe and Y. Teraoka, *Jpn. J. Appl. Phys.* **49**, 115704 (2010).
- <sup>26</sup>A. Yoshigoe and Y. Teraoka, *J. Phys. Chem. C* **114**, 22539 (2010).
- <sup>27</sup>A. Yoshigoe and Y. Teraoka, *J. Phys. Chem. C* **118**, 9436 (2014).
- <sup>28</sup>D. Schmeisser, R. D. Schnell, A. Bogen, F. J. Himpsel, D. Rieger, G. Landgren, and J. F. Morar, *Surf. Sci.* **172**, 455 (1986).
- <sup>29</sup>H. J. Kuhr and W. Ranke, *Surf. Sci.* **201**, 408 (1988).
- <sup>30</sup>M. L. Yu and L. A. DeLouise, *Surf. Sci. Rep.* **19**, 285 (1994).

- <sup>31</sup>*The Chemical Physics of Solid Surfaces: Surface dynamics*, edited by D. Woodruff (Elsevier, Amsterdam, 2003).
- <sup>32</sup>Y. Teraoka and A. Yoshigoe, *Jpn. J. Appl. Phys.* **41**, 4253 (2002). In this reference, multiplication by 0.76 is necessary to correct translational energies.
- <sup>33</sup>Y. Saitoh, Y. Fukuda, Y. Takeda, H. Yamagami, S. Takahashi, Y. Asano, T. Hara, K. Shirasawa, M. Takeuchi, T. Tanaka, and H. Kitamura, *J. Synchrotron Radiat.* **19**, 388 (2012).
- <sup>34</sup>K. Prabhakaran and T. Ogino, *Surf. Sci.* **325**, 263 (1995).
- <sup>35</sup>D. R. Miller, *Atomic and Molecular Beam Methods*, edited by G. Scoles (Oxford University Press, Oxford, 1988).
- <sup>36</sup>H. Pauly, *Atom, Molecule, and Cluster Beams* (Springer-Verlag, Berlin, 2000).
- <sup>37</sup>M. D. Morse, *Atomic, Molecular, and Optical Physics: Atoms and Molecules*, edited by F. B. Dunning and R. G. Hulet (Academic Press, London, 1996).
- <sup>38</sup>The translational energy of O<sub>2</sub> in a seeded molecular beam is  $E_t = S^2 RT_n m_{O_2}/m$  where we assume ideal gas behavior including zero velocity slip via adiabatic-expansion. In this equation,  $R$ ,  $T_n$ ,  $m_{O_2}$ , and  $m$  indicate the gas constant, nozzle temperature, oxygen molecular weight, and mean molecular weight of mixed gas, respectively.  $S = M \sqrt{\frac{\gamma}{2+(\gamma-1)M^2}}$ , where  $\gamma$  is the specific heat ratio ( $= 5/3$ ). In this study, we assumed that the Mach number ( $M$ ) was 10.
- <sup>39</sup>K. Moritani, M. Okada, Y. Teraoka, A. Yoshigoe, and T. Kasai, *J. Phys. Chem. A* **113**, 15217 (2009).
- <sup>40</sup>We found that the uptake curve was strongly influenced by surface impurities such as C and Mo. Actually, the initial sticking probability was one order of magnitude smaller when C or Mo was detected by SR-XPS. One possible reason for this suppression might be the surface electronic structure changes of the Ge(100)-2 × 1 surface because of the presence of impurities.
- <sup>41</sup>F. J. Himpsel, F. R. McFeely, A. Taleb-Ibrahimi, J. A. Yarmoff, and G. Hollinger, *Phys. Rev. B* **38**, 6084 (1988).
- <sup>42</sup>P. E. J. Eriksson and R. I. G. Uhrberg, *Phys. Rev. B* **81**, 125443 (2010).
- <sup>43</sup>H. W. Yeom, H. Hamamatsu, T. Ohta, and R. I. G. Uhrberg, *Phys. Rev. B* **59**, R10413 (1999).
- <sup>44</sup>A. Yoshigoe and Y. Teraoka, *Surf. Sci.* **532–535**, 690 (2003). In this reference, multiplication by 0.76 is necessary to correct translational energies and the data for 0.04 eV corresponds to that of thermal-O<sub>2</sub>.
- <sup>45</sup>A. Goldoni, S. Modesti, V. R. Dhanak, M. Sancrotti, and A. Santoni, *Phys. Rev. B* **54**, 11340 (1996).
- <sup>46</sup>S. R. M. da Silva, G. K. Rolim, G. V. Soares, I. J. R. Baumvol, C. Krug, L. Miotti, F. L. Freire, Jr., M. E. H. M. da Costa, and C. Radtke, *Appl. Phys. Lett.* **100**, 191907 (2012).
- <sup>47</sup>D. E. Starr, Z. Liu, M. Hävecker, A. Knop-Gericke, and H. Bluhm, *Chem. Soc. Rev.* **42**, 5833 (2013).
- <sup>48</sup>K. Kato, T. Uda, and K. Terakura, *Phys. Rev. Lett.* **80**, 2000 (1998).
- <sup>49</sup>J. Behler, K. Reuter, and M. Scheffler, *Phys. Rev. B* **77**, 115421 (2008).
- <sup>50</sup>U. Khalilov, G. Pourtois, A. C. van Duin, and E. G. Neyts, *J. Phys. Chem. C* **116**, 8649 (2012).